

## Development of coal tar-free coatings: Acetylated lignin as a bio-additive for anticorrosive and UV-blocking epoxy resins

Otilio B.F. Diógenes<sup>a</sup>, Davi R. de Oliveira<sup>b</sup>, Lucas R.R. da Silva<sup>a</sup>, Ítalo Gomes Pereira<sup>c</sup>, Selma Elaine Mazzetto<sup>b</sup>, Walney S. Araujo<sup>a</sup>, Diego Lomonaco<sup>b,\*</sup>

<sup>a</sup> Department of Metallurgical and Materials Engineering, Federal University of Ceara, 60440-900 Fortaleza-CE, Brazil

<sup>b</sup> Department of Organic and Inorganic Chemistry, Federal University of Ceara, 60440 900 Fortaleza-CE, Brazil

<sup>c</sup> Department of Chemical Engineering, Federal University of Ceara, 60440-900 Fortaleza-CE, Brazil

### ARTICLE INFO

#### Keywords:

Lignin  
Epoxy coating  
Coal tar-free  
Corrosion protection

### ABSTRACT

Coal tar epoxy (CTE) coatings promote effective protection of steel structures under critical conditions of atmosphere and immersion. However, according to the international guideline, coal tar has been reported as a mutagenic and carcinogenic compound and has been prohibited for use in countries such as the USA and Japan. Aiming to replace the use of CTE coatings, this paper proposes the use of Kraft lignin, a bio-polyphenol considered safe and obtained as waste from the pulp and paper industry, to develop a coal tar free epoxy coating. In order to promote better compatibilization with bisphenol A diglycidyl ether (DGEBA), lignin was subjected to the acetylation process. The epoxy-lignin resin was obtained by incorporating acetylated lignin into DGEBA. Three types of epoxy-lignin resin were prepared, namely: DGEBA/7.5% lignin, DGEBA/15% lignin and DGEBA/30% lignin. The chemical structure of the resin was evaluated by Fourier transform infrared spectroscopy (FTIR). For the coating preparation, the resin was cured using isophorone diamine (IPDA). The resultant thermosetting were analyzed regarding their chemical, thermal, anticorrosive and UV-blocking properties using the DGEBA and CTE coatings as reference. The anticorrosive properties of the coatings were evaluated by electrochemical impedance spectroscopy (EIS). The adhesion of the coatings was evaluated by the pull-off method (ASTM D4541). A complete absorption of UV light in the UV-A and UV-B regions was observed in the coatings add with acetylated lignin, a property very valuable in order to prevent the UV damage and the durability reduction of epoxy coatings. EIS results showed that the epoxy-lignin coatings (with 7.5 and 15% lignin content) presented modulus of impedance values comparable to the commercial coating and superior to the CTE coating, indicating the potential use of this coating as a corrosion protector.

### 1. Introduction

Many strategies have been adopted in order to protect metals against corrosive processes triggered by aggressive environmental factors such as humidity, O<sub>2</sub>, Cl<sup>-</sup> ions and others. Among them, the use of organic coatings stands out due to their barrier effects that act effectively isolating materials from corrosive species and extending their useful life [1].

In this context, epoxy resins attract special attention in the development of anticorrosive organic coatings compared to other synthetic resins, due to their low cost, low shrinkage, good dimensional stability and high mechanical, chemical and adhesive properties [1,2]. However, the anticorrosive ability of epoxy coatings weaken during long periods

of exposure depending on the environment due to solar radiation, wet-dry cycling, and high salinity [3]. Therefore, it is a crucial issue to develop strategies in order to improve the service life of epoxy coatings.

The use of coal tar-based epoxy coatings (CTE) to protect against corrosion of underground pipes and steel structures have been used for more than a century. This protection is possible because epoxy resins with coal tar have extremely low permeability, high electrolytic resistance and good adhesion, even on surfaces that have not been well prepared, enabling their use in extremely severe environments, such as the marine, especially in submerged areas [4].

However, the mixture of polycyclic aromatic hydrocarbons present in the coal tar composition are bio-accumulative, toxic to the environment, and have carcinogenic activity, which led the International

\* Corresponding author.

E-mail address: [lomonaco@ufc.br](mailto:lomonaco@ufc.br) (D. Lomonaco).

<https://doi.org/10.1016/j.porgcoat.2021.106533>

Received 1 May 2021; Received in revised form 19 August 2021; Accepted 15 September 2021

Available online 23 September 2021

0300-9440/© 2021 Elsevier B.V. All rights reserved.

Agency for Research on Cancer (IARC) to categorize as Group 1 carcinogens formulations containing more than 5% of the raw coal tar [5,6]. These facts points to a possible ban of coal tar-based paint products.

In view of this, it is necessary to find substitute materials to coal tar for the synthesis of more environmentally safe and healthier organic coatings. Alternative approaches, such as the use of bitumen and functionalized hydrocarbon resins have been proposed [4]. But there is still a lack in the literature about natural products that can replace the coal tar. In this context lignin stands out as a widely available aromatic compound that represents an interesting potential alternative.

Lignin is a natural polyphenol and one of the three main constituents of the so-called lignocellulosic biomass, together with cellulose and hemicellulose. It is the second most abundant material in the vegetable kingdom (after cellulose) and the largest natural and renewable source of aromatic compounds [7]. Kraft lignin is the name given to lignin obtained by Kraft process. Approximately 55 million tonnes of Kraft lignin are produced as a by-product of paper and pulping industry, being normally burned in industrial furnaces and boilers for energy production, which represents an undervaluation of this material [8].

Due to the presence of aromatic rings in its polymeric structure, lignin is expected to be a good alternative to petroleum-based chemicals [9]. Its phenylpropanoid structure and the high content of diverse functional groups (carbonyls, carboxyls, phenolic and aliphatic hydroxyls) allows the use of lignin as a neutralizer or inhibitor in the oxidation processes, by means of the stabilizing reactions induced by oxygen radicals and their respective species [10].

Lignin has also a remarkable ability to act as a blocker of ultraviolet radiation due to the large number of phenolic units, ketones, and other chromophores presents in its structure, which combined with the aromatic rings, are capable to form large conjugated  $\pi$  systems, which are capable of absorbing UV radiation [11–14]. This property can become especially interesting for its use as a potential additive for epoxy resins, since it is known that epoxy resins are susceptible to degradation when exposed to UV radiation and have their durability substantially reduced when used in outdoors environments [15].

However, due to a large number of hydroxyl groups present in the lignin structure, which are centers of high polarity and may hamper their interaction with nonpolar polymers, direct incorporation of lignin in polymeric matrices can be difficult. In this sense, chemical modifications of hydroxyl groups of lignin have been employed as strategies to overcome this problem. Among many modifications proposed in literature, lignin acetylation has been performed for decades and is one of the most widespread chemical modifications used to improve the solubility of this biopolymer in organic solvents and increase polymer-lignin compatibility [16,17].

In a previous work [18], our group has demonstrated that PMMA films incorporated with acetylated lignin presented the initial degradation temperature ( $T_{onset}$ ) values higher than PMMA films incorporated with unmodified lignin, suggesting that acetylation contributes to an enhancement of thermal stability. Furthermore, acetylated lignin is expected to be able to maintain its ability to act as a UV-blocker, since the acetyl groups also have  $\pi$  electrons that are capable of absorbing UV radiation.

In view of the undesirable effects of coal tar on human health and environment, and the attractive characteristics of lignin as a sustainable alternative to petrochemicals, this work aims to develop an epoxy resin added with acetylated lignin that presents UV-blocking properties and corrosion protection characteristics comparable or superior to epoxy resins with coal tar.

## 2. Materials and methods

### 2.1. Materials

Kraft lignin (KL) was gently supplied by Suzano Papel e Celulose.

Acetic anhydride (98%) and ethyl acetate were used as received from LabSynth (Brazil). Bisphenol A diglycidyl ether resin (DGEBA) and isophorone diamine (IPDA) were purchased from Fortcolor Tintas (Brazil). CTE coating was purchased from Planquímica.

### 2.2. Lignin acetylation

Lignin acetylation was performed following the general procedure described by Oliveira et al. [18] with minor modifications. To this, Kraft lignin (15 g) was dissolved in acetic anhydride (45 mL) in a 250 mL round-bottom flask equipped with a stirring bar. After dissolution, the mixture was placed in the microwave reactor (StartSYNTH) operating at a power of 850 W for 25 min, of which 5 min were to reach the temperature of 120 °C and, when reached this temperature, the mixture remained in it for 20 min. After heating in the microwave, the mixture was poured into water (100 mL), stirred during 1 h, and reserved for approximately 12 h for the lignin precipitation. After this time, the mixture was filtered and washed with distilled water until the washing water had a neutral pH. Then, the lignin was dried in an oven at 105 °C during 1 h to remove traces of water. To analyze the efficiency of the acetylation process, an infrared spectroscopy (FTIR) analysis was performed on lignin. At the end of the process, an ethyl acetate soluble lignin was obtained to be used in the preparation of the coating.

### 2.3. Coating preparation

Table 1 shows the quantity of reagents used in the preparation of epoxy/lignin coatings.

Initially, using the magnetic stirrer, the lignin was dissolved in ethyl acetate. Then, the mixture was added to the DGEBA epoxy resin and concentrated under reduced pressure to eliminate part of the solvent and acquire the desired viscosity.

### 2.4. Surface preparation

SAE 1020 carbon steel plates with dimensions 15 cm  $\times$  10 cm  $\times$  0.3 cm were used as a metallic substrate.

The steel plates went through the cleaning process by abrasive blasting with steel shot to eliminate oxide residues. Then, the samples were subjected to an acetone bath for degreasing.

After cleaning the plates, the roughness profile of the specimens was measured using the PosiTector SPG digital surface roughness meter. The average value of the roughness of the samples was 22.96  $\mu\text{m}$   $\pm$  5.35  $\mu\text{m}$ .

### 2.5. Applying the coating to the substrate

The application of the coating was done using a 2" paintbrush. The curing of the coatings was carried out at room temperature for 168 h.

After curing process, the thickness of the coatings was measured with the aid of the PosiTector®6000 coating thickness gauge. Eight measurements were made in each sample and the average value was considered as the final thickness. The measured thicknesses are shown in Table 2.

**Table 1**  
Reagents used in the production of coatings.

Coating	Mass of lignin (g)	Mass of DGEBA (g)	Volume of ethyl acetate (mL)
DGEBA/7.5% LIG.	7.5	92.5	37.5
DGEBA/15% LIG.	15	85	75
DGEBA/30% LIG.	30	70	150

**Table 2**  
Average coating thickness.

Coating	Thickness ( $\mu\text{m}$ )	Standard deviation ( $\mu\text{m}$ )
DGEBA	352.83	95.49
DGEBA/7.5% LIG.	350.46	86.98
DGEBA/15% LIG.	376.23	101
DGEBA/30% LIG.	305.98	83.73
CTE	311.30	82.75

## 2.6. Characterization techniques and test methods

### 2.6.1. FTIR

The characterization of the of lignin samples and cured coatings were carried out from the FTIR spectrum, obtained in a Perkin Elmer spectrophotometer model FT-IR/NIR FRONTIER, using an attenuated total reflectance (ATR) accessory with zinc selenide crystal (ZnSe) in transmittance mode. The range of the spectra were constructed using 32 scans between 4000 and 500  $\text{cm}^{-1}$  with a resolution of 4  $\text{cm}^{-1}$ .

### 2.6.2. TGA

The thermal behavior of of KL, AKL and cured coatings were studied by Thermogravimetric Analysis (TGA, Mettler-Toledo TGA/SDTA851e). For analysis, 5 mg of each coating was added to an alumina crucible. The samples were submitted to a heating program, in which the temperature varied from 30 to 800  $^{\circ}\text{C}$ , at a heating rate of 10  $^{\circ}\text{C}/\text{min}$  under an atmosphere of  $\text{N}_2$  with a purge of 50 mL/min.

### 2.6.3. DSC

The glass transition temperature of the coatings was evaluated by means of differential scanning calorimetry (DSC) analysis. The DSC thermograms were obtained in a Mettler-Toledo equipment, model DSC 823e. The analyzes were conducted under an  $\text{N}_2$  atmosphere (flow of 50 mL/min), using approximately 5 mg of the samples, which were initially heated to 25 to 60  $^{\circ}\text{C}$ , then cooled to 60 to  $-20^{\circ}\text{C}$  and then heated again from  $-20$  to 150  $^{\circ}\text{C}$ . The glass transition temperature ( $T_g$ ) was defined as the midpoint of the change in heat capacity in the last heating cycle. All analyzes were performed using platinum melting pot.

### 2.6.4. UV protection

The optical properties of the coatings were investigated using the Cary 60 spectrophotometer (Agilent Technologies) in the range 200 to 700 nm with a spectral resolution of 0.5 nm. The evaluation of the UV protection capacity of epoxy-lignin coatings was determined using their transmittance in the ranges from 280 to 320 nm (UV-B) and from 320 to 380 nm (UV-A). The AKL UV absorption spectrum was obtained using a lignin solution (5 mg  $\text{mL}^{-1}$  in DMSO) analyzed in a wavelength range from 400 to 250 nm using a spectral resolution of 0.1 nm.

### 2.6.5. Electrochemical impedance spectroscopy

The electrochemical impedance spectroscopy (EIS) technique was used to evaluate the corrosion protection performance of working electrodes during immersion in a 3.5% (w/v) NaCl solution at room temperature. The tests were carried out in a potentiostat/galvanostat of the Autolab model PGSTAT302N and the tests were read using the software NOVA 2.1. Metallic substrates coated with commercial varnish (DGEBA) and CTE coating were used as control samples for comparative purposes. EIS measurements were performed based on the open circuit potential after 0.5 h immersion in NaCl solution. Measurements were taken at the following immersion times: 0.5, 5, 24, 48, 120 and 168 h.

A conventional electrochemical cell with three electrodes was used in the measurements, these electrodes being: I - Reference electrode: Ag (s)/AgCl (s)/Cl $^{-}$  (aq) (saturated KCl); II - Counter electrode: platinum plate; and III - Working electrode: metallic carbon steel substrates covered with CTE, DGEBA and DGEBA with different concentrations of lignin. The electrolyte used was the 3.5% NaCl solution at room

temperature. The area of the working electrodes in contact with the electrolyte was delimited by the area of the acrylic cell that made up the electrochemical cell, which is 19,6  $\text{cm}^2$ . A sinusoidal potential disturbance of 15 mV was applied in the 10 $^5$  Hz - 6  $\times$  10 $^{-3}$  Hz frequency range.

### 2.6.6. Adhesion test

The paint adhesion test on the substrate was evaluated using the pull-off method (ASTM D4541). The equipment for performing the test was the PosiTest AT-A Automatic Adhesion Tester (DeFelsko - Type V model).

ISO 4624 classifies the failures of the Pull Off test as adhesive or cohesive. Adhesive failures happen in two situations: when the film is completely detached from the metallic substrate or when the paint is partially removed. Cohesive failure occurs when the paint does not detach from the substrate, with a break within the paint layer itself.

For the test, three samples of each coating were used. At the end of the test, both the tensile strength and the type of failure values are the averages of these three samples. In this work, the percentage of the types of failures resulting from the adhesion test was estimated by using the free software ImageJ to calculate the areas related to each type of failure.

## 3. Results

### 3.1. Structural characterization by Fourier transform infrared spectroscopy (FTIR) and Thermogravimetric Analysis (TGA) of Kraft lignin and acetylated Kraft lignin

Due to the large number of hydroxyl groups present in the lignin structure, their compatibility in polymeric matrices can be challenging, since these groups constitute centers of polarity and may hamper interactions with non-polar polymers. As a strategy to improve lignin-polymers compatibility, esterification of hydroxyl groups has been widely used [17–19].

In this work, acetylation of hydroxyl groups was performed through a fast and simple microwave-assisted process [18] in order to improve the compatibility DGEBA-lignin. In Fig. 1 the FTIR spectra of unmodified Kraft lignin (KL) and acetylated Kraft lignin (AKL) are compared.

In the FTIR spectrum of KL, a broad band centered at approximately 3440  $\text{cm}^{-1}$  can be observed, which is attributed to the stretching of the O–H bonds of the hydroxyl groups present in the lignin. It is also possible to observe the bands attributed to the stretching of the connections = C–H and C–H (2937 and 2841  $\text{cm}^{-1}$ , respectively) as well as bands characteristic of the stretching of aromatic C = C connections (1596, 1511, 1460 and 1426  $\text{cm}^{-1}$ ) [17,20].

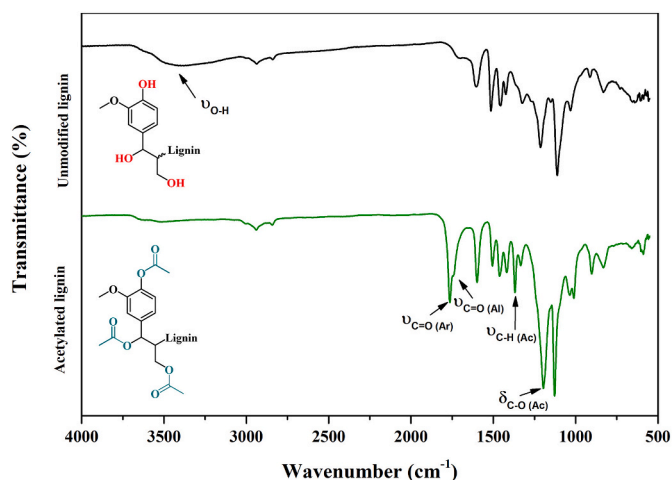


**Fig. 1.** FTIR spectrum of unmodified Kraft lignin (KL) and acetylated Kraft lignin (AKL).

In the FTIR spectrum of AKL, two main evidences suggest the acetylation of the hydroxyl groups: (1) the great decrease in the intensity of the broadband attributed to the stretching of the OH bonds in  $3440\text{ cm}^{-1}$ , almost disappearing, and (2) the appearance of two new bands in  $1764$  and  $1741\text{ cm}^{-1}$ , which are attributed to the stretching of  $\text{C}=\text{O}$  bonds in aromatic and aliphatic esters, respectively ( $\nu_{\text{C}=\text{O}(\text{Ar})}$  and  $\nu_{\text{C}=\text{O}(\text{Al})}$ ) in Fig. 1 [18,21].

A band at  $1366\text{ cm}^{-1}$ , which can be attributed to the stretching of the  $\text{C}-\text{H}$  bond in acetyl groups, and a band at  $1196\text{ cm}^{-1}$ , which is attributed to the deformation of the  $\text{C}-\text{O}$  bond of the acetyl groups, are also observed ( $\nu_{\text{C}-\text{HAc}}$  and  $\delta_{\text{C}-\text{OAc}}$ ) in Fig. 1 [21].

Thus, the appearance of the bands in  $1764$  and  $1741\text{ cm}^{-1}$  accompanied by the expressive decrease of the band in  $3440\text{ cm}^{-1}$  is indicative of the acetylation of the aliphatic and aromatic hydroxyl groups present in lignin.

In order to evaluate the thermal behavior of acetylated kraft lignin when compared to unmodified lignin, thermogravimetric analysis (TGA) was performed. In Fig. 2 the TGA and DTGA curves of KL and AKL are shown. The initial degradation temperatures ( $T_{\text{onset}}$ ) and maximum degradation ( $T_{\text{max}}$ ), as well as the ash content (CY) of each sample are summarized in Table 3.

As can be seen in TGA thermograms (Fig. 2), both samples presented similar degradation profiles, with a small change in the hydrophilicity of AKL, as shown by the lower mass loss below  $100\text{ }^{\circ}\text{C}$ . This behavior can be attributed to the substitution of hydroxyl groups in KL by acetyl groups in AKL, reducing the interaction of lignin with atmospheric humidity, making AKL more hydrophobic.

Table 3 shows that acetylation also promoted a slight enhancement in  $T_{\text{onset}}$  (rising from  $283\text{ }^{\circ}\text{C}$  for KL to  $287\text{ }^{\circ}\text{C}$  for AKL) and  $T_{\text{Max}}$  (rising from  $370\text{ }^{\circ}\text{C}$  for KL to  $379\text{ }^{\circ}\text{C}$  for AKL). The main degradation event observed for both samples, between  $200$  and  $500\text{ }^{\circ}\text{C}$ , is associated with the fragmentation of interunit linkages, as for example the ether linkages between aromatic units. Table 3 also shows that acetylation promoted a considerable increase in CY (rising from  $26.2\%$  for KL to  $34.6\%$  for AKL), which is a desirable characteristic for a possible polymer additive, since high ash contents contribute to the flame resistance of a polymer [22,23].

Thus, in a general sense, the results presented by TGA analysis show that acetylation of KL promoted a slight improvement in the thermal stability of this natural polymer and increase their char yield, which can be attractive to enhance the flame resistance of a material, making AKL

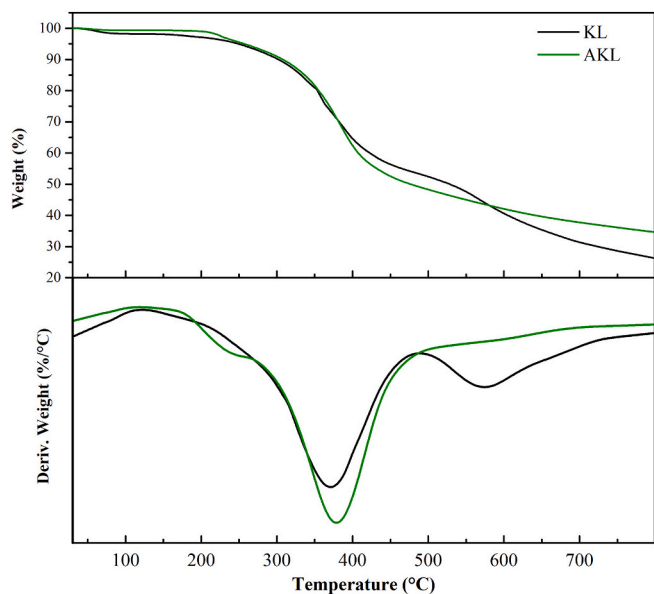


Fig. 2. TGA and DTGA curves of unmodified kraft lignin (KL) and its acetylated kraft lignin (AKL).

Table 3

TGA data for KL and AKL.

Sample	$T_{\text{onset}}\text{ (}^{\circ}\text{C)}$	$T_{\text{Max}}\text{ (}^{\circ}\text{C)}$	CY (%)
KL	283	370	26.2
AKL	287	379	34.6

attractive to be used as a potential bio-additive for polymers.

### 3.2. Structural characterization by Fourier Transform Infrared Spectroscopy (FTIR) of coatings

In Fig. 3, the FTIR spectra of the commercial coating with the coatings with the addition of lignin, after curing at room temperature for seven days, are compared, in the  $1800$  to  $550\text{ cm}^{-1}$  region.

It was possible to observe that the spectra of the DGEBA, DGEBA/7.5% lignin and DGEBA/15% lignin coatings were similar, indicating that the addition of lignin in the concentrations of 7.5% and 15% did not harm the curing process of the coatings, since the band attributed to the  $\text{C}-\text{O}$  bond of the epoxy ring ( $914\text{ cm}^{-1}$ ) was not observed. The spectrum of the DGEBA/30% lignin coating, however, showed the band at  $914\text{ cm}^{-1}$ , being an indication of inefficiency in the resin curing process [24].

### 3.3. TGA

The thermal stability of the cured coatings was determined from the statistical index of heat resistance (Ts). This index was calculated according to Eq. (1) [25].

$$T_s = 0.49[T_{d5\%} + 0.6(T_{d30\%} - T_{d5\%})] \quad (1)$$

where  $T_{d5\%}$  is the temperature value corresponding to 5% of mass loss and  $T_{d30\%}$  is the temperature value corresponding to 30% of mass loss of coatings. Both values were determined from the temperatures measured in the TGA test.

The TGA results and DTG curves for the coatings studied are shown in Fig. 4.

An increase in residual mass ( $R_{800}$ , Table 4) was observed with an increase in the concentration of lignin in the coatings (Table 4). This behavior was already expected, since lignin favors the formation of a carbonaceous structure through condensation of aromatic rings under high temperatures [26]. Furthermore, the addition of 30% lignin to the epoxy coating was sufficient to match the residual mass value of the CTE coating, which makes the addition of AKL lignin attractive to be used as

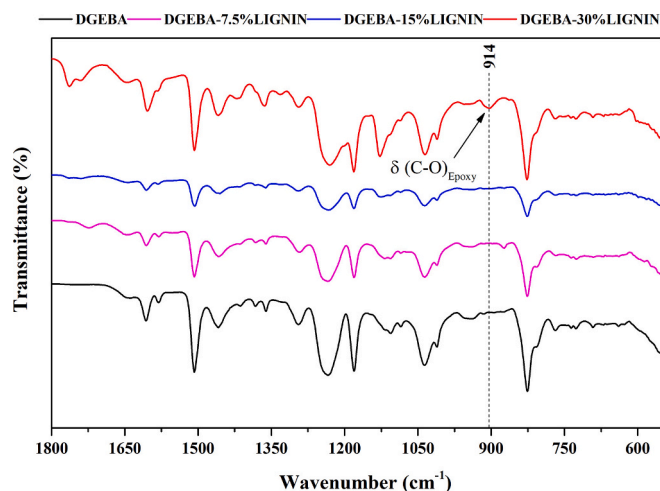


Fig. 3. FTIR spectrum of the DGEBA, DGEBA/7.5% lignin, DGEBA/15% lignin and DGEBA/30% lignin coatings.

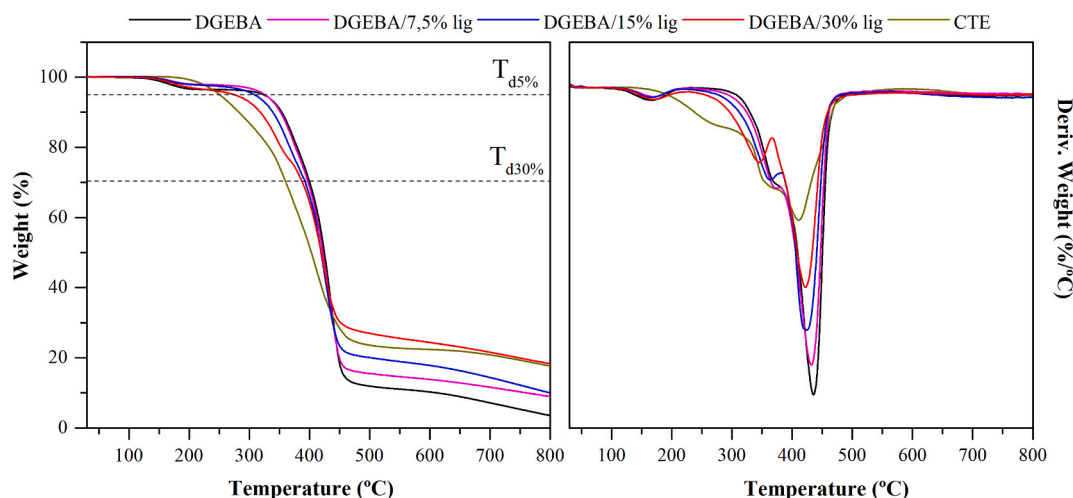


Fig. 4. TGA and DTG curves for the DGEBA, DGEBA/7.5% lignin, DGEBA/15% lignin, DGEBA/30% lignin and CTE coatings.

Table 4

Thermal decomposition data of the studied coatings.

Coating	R <sub>800</sub> * (%)	T <sub>onset</sub> (°C)	T <sub>p</sub> (°C)	T <sub>d5%</sub> (°C)	T <sub>d30%</sub> (°C)	T <sub>s</sub> (°C)
DGEBA	3.5	341	436	323	400	182
CTE	17.6	222	411	250	360	154
DGEBA/7.5% lig.	8.9	336	432	325	397	180
DGEBA/15% lig.	10	323	422	307	392	175
DGEBA/30% lig.	18.3	308	422	274	387	167

\* R<sub>800</sub>: residual mass at 800 °C.

a bio-additive.

Through the DTG curve, it was observed that all coatings containing DGEBA/lignin or neat DGEBA presented two-stage degradation profiles. The first stage is in the temperature range of 120–207 °C, which can be attributed to the volatilization of residual solvent present in the coating, while the second, in the range of 245–500 °C, can be related to the fragmentation of macromolecules [27,28].

The thermal decomposition of neat DGEBA occurred in a single step in the temperature range of 300–475 °C with the highest rate of decomposition (T<sub>p</sub>) around 436 °C. These results are in agreement with the results obtained in the literature [28].

In general, the epoxy resin added with lignin showed better thermal performance than the CTE coating. However, comparing the degradation onset temperatures (T<sub>onset</sub>) to the pure DGEBA coating there was a reduction of 1.4% which was observed for the DGEBA/7.5% lignin coating, 5.2% for the DGEBA/15% lignin coating and 9.6% for the coating of DGEBA/30% lignin (Table 4).

The same behavior is seen through the calculation of the statistical index of heat resistance (T<sub>s</sub>), a small variation was observed between the values calculated for coatings with lignin addition to the DGEBA coating (Table 4).

This decrease may be related to the presence of more thermally degradable lignin molecules and readily cleavable ether bonds, which anticipate the T<sub>onset</sub> of the lignin coatings [25,29].

### 3.4. DSC

The glass transition temperature (T<sub>g</sub>) of the coatings was evaluated using differential scanning calorimetry (DSC). The non-isothermal DSC thermograms of coatings containing different concentrations of lignin are shown in Fig. 5.

Through the DSC thermograms it is observed that, with the increase

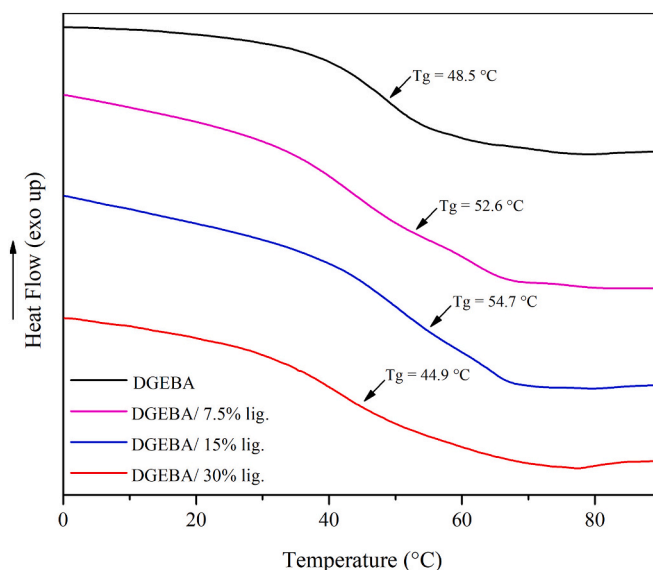


Fig. 5. DSC analysis for DGEBA, DGEBA/7.5% lignin, DGEBA/15% lignin and DGEBA/30% lignin coatings.

of the lignin concentration in the coatings from 0% to 15%, there was an increase in the T<sub>g</sub> values, going from 48.5 °C to 54.7 °C. A higher concentration of lignin (30%), however, caused a decrease in the T<sub>g</sub> value of the coating to 44.9 °C.

Higher T<sub>g</sub> values may indicate a higher crosslink density of the polymeric material. As it is a solid material and due to its inhomogeneous structure, it was already expected that the addition of lignin would lead to the formation of a more rigid structure, consequently increasing the T<sub>g</sub> values.

The decrease in the T<sub>g</sub> value in the coating containing 30% lignin is the result of an inefficient reaction of opening the epoxy rings, as observed through the FTIR spectra of the coatings (Fig. 3), where it was possible to notice that the band attributed to the C—O bond of the epoxy ring (914 cm<sup>-1</sup>) still remains visible. The high concentration of lignin can lead to its partial agglomeration in the coating, resulting in an inefficient crosslinking compared to coatings with a lower lignin content [25].

### 3.5. UV protection

Epoxy resins have several excellent properties for their use as coatings, including high thermal stability, good chemical resistance, low permeability, high electrolytic resistance and good adhesion. However, when exposed to the incidence of UV radiation, these resins tend to undergo degradation, affecting their chemical, physical and mechanical properties. UV blockers have been used as a way to overcome this drawback, decreasing the rate of UV degradation [15,30].

Due to the lignin structure, which presents a great amount of phenolic hydroxyls groups combined to a conjugated  $\pi$  system from the aromatic rings that can absorb the UV light, this biopolymer have been used as an UV absorber additive in different types materials, preventing them degradation and aging [11].

Fig. 6 shows the UV absorption spectrum of AKL. As can be seen, acetylated lignin has absorption capacity across the entire range of UV radiation. The acetylation of the phenolic hydroxyl groups did not compromise the UV absorption capacity of AKL, since the acetyl groups also have  $\pi$  electrons that are capable to form conjugated  $\pi$  systems with aromatic rings presents in the lignin structure, absorbing UV radiation.

Fig. 7 shows the UV-Vis spectra of neat DGEBA coating and DGEBA-lignin coatings with the main UV regions highlighted.

The analysis of Fig. 7 makes evident the UV absorption capacity provided by lignin addition to the coatings. Neat DGEBA coating has a poor ability to absorb the UV-A and UV-B light, transmitting radiation in those regions. The incorporation of AKL provided full UV protection to the coatings, since all the epoxy-lignin coatings were capable to absorbing the whole UV light in both UV-A and UV-B region of the spectra.

It is worth to note that even the lowest concentration of AKL (DGEBA/7.5% lig) already reached full UV light absorption. In previous works [31,32] a synergistic effect was observed between lignin and other chemical components present in sun protection lotions, which led to an expressive increase in the UV absorption capacity. This effect is probably induced by the  $\pi - \pi^*$  stacking interactions between the aromatic rings of lignin and the active compounds present in the lotions. Thus, it is reasonable to assume that the same type of  $\pi - \pi^*$  stacking interaction can occur between the aromatic rings of lignin and the aromatic rings of DGEBA, forming systems that can absorb photons in the UV region to carry out  $\pi - \pi^*$  transitions.

Therefore, the use of acetylated lignin as a bio-additive to epoxy coatings proved to be an interesting strategy to give UV protection properties to these materials, making them more resistant to photo-degradation, increasing their durability and making them more suitable

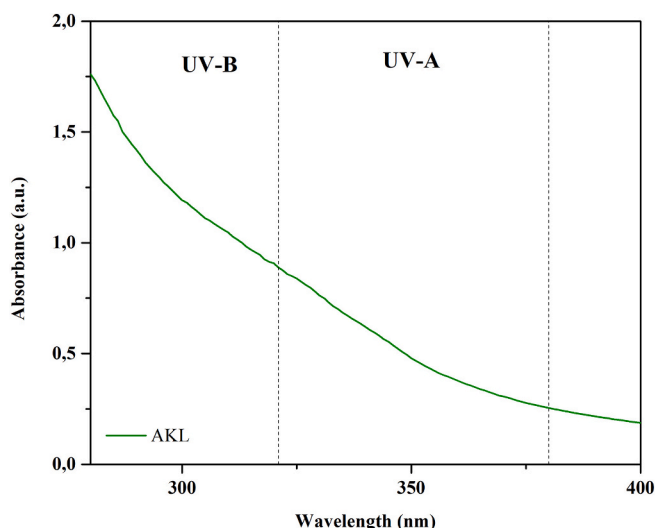


Fig. 6. UV absorption spectrum of AKL.

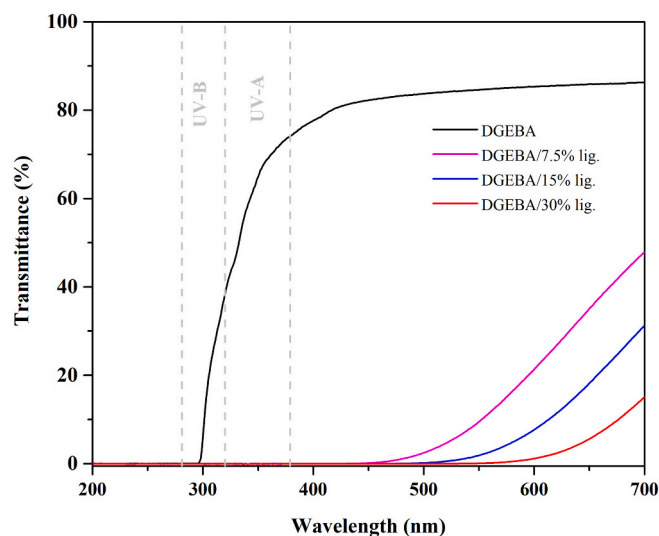


Fig. 7. UV-Vis spectra of coatings DGEBA, DGEBA/7.5% lignin, DGEBA/15% lignin and DGEBA/30% lignin.

for applications that require exposure to UV radiation.

### 3.6. EIS

The impedance measurements obtained after 7 days of immersion in 3.5% NaCl solution at room temperature are shown in Fig. 8. The values of modulus of impedance obtained from the Bode diagram at the lowest frequency ( $|Z|_{f=0.006}$ ) are presented in Table 5. This value could be used as a semi-quantitative indicator of the barrier performance of the coating [33].

Fig. 8 shows that coatings DGEBA, DGEBA/7.5% lignin and DGEBA/15% lignin showed values of  $|Z|$  superior to  $10^{11} \Omega \cdot \text{cm}^2$ , while the DGEBA/30% lignin and CTE coatings presented  $|Z|$  two orders of magnitude lower. Although only one immersion test for 7 days does not bring enough information to classify the properties of the coatings [34], it allows us to observe that the DGEBA/30% lignin and CTE coating showed worse electrochemical performance than the others did. It was also possible to observe that the additions of 7.5% and 15% of lignin did not significantly changed the performance of the DGEBA resin, since the values of  $|Z|$  remained close to the commercial resin (Table 5). This result can be attributed to the high barrier property of lignin [33].

A phase angle close to  $-90^\circ$  indicates that the coating has a capacitive behavior, as it has high values of resistance and/or capacitance and this fact makes the current flow mainly through the capacitor [35]. From the - phase angle vs  $\log f$  graph (Fig. 8), it is possible to observe that the coatings DGEBA, DGEBA/7.5% lignin and DGEBA/15% lignin presented constant phase angle values very close to  $-90^\circ$  in the range  $40-10^5$  Hz, indicating a capacitive behavior in this frequency range. While in the frequency range of  $6 \times 10^{-3} - 40$  Hz, there was a behavior of decreasing the phase angle, which may be associated with the decrease in resistance and/or capacitance of the coating, causing the current to also flow through the resistor. This fact characterizes a resistive/capacitive (RC) behavior of the coating. This behavior is reported as characteristic of a high-quality coating. The DGEBA/30% lignin and CTE coatings showed a capacitive behavior in a lower frequency range than the others coatings ( $4 \times 10^3 - 10^5$  Hz and  $10^4 - 10^5$  Hz, respectively) and an RC behavior in the ranges of  $6 \times 10^{-3} - 4 \times 10^3$  and  $6 \times 10^{-3} - 10^4$ , respectively. This Bode plot model is associated with an intermediate quality coating [36].

The EIS data were analyzed using the equivalent electrical circuit (EEC) models represented in Fig. 9. These two models are generally used to represent the electrical behavior of a coated carbon steel exposed to an electrolyte, where  $R_s$  represents the resistance of the solution/electrolyte,  $R_c$  the polarization resistance of the coating and  $C_c$  is the coating

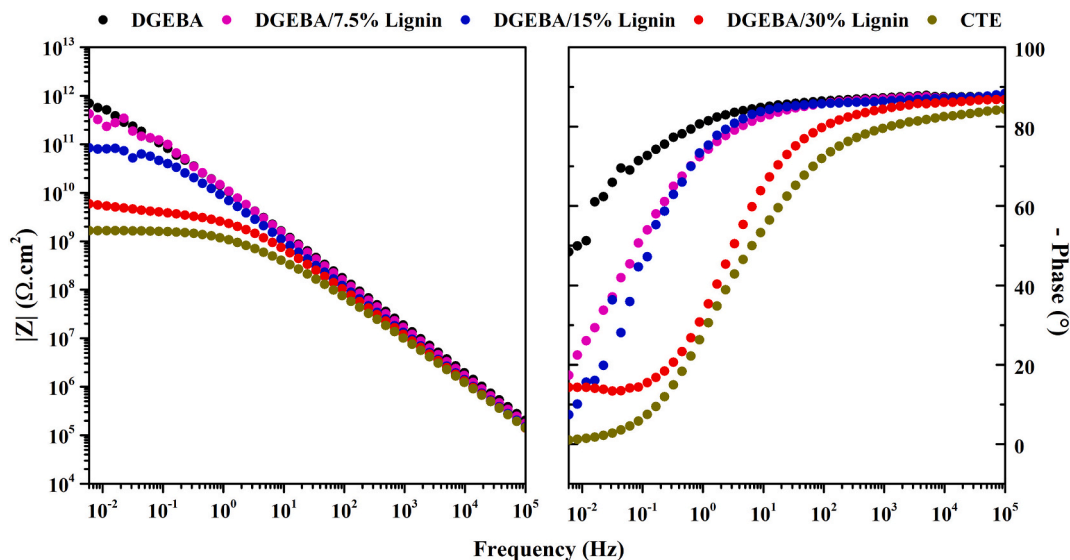


Fig. 8. Bode Plots of coatings after 1 week immersed in NaCl 3.5% at room temperature.

Table 5

Average values of  $|Z|$  at low frequency (0.006 Hz) after 7 days of immersion.

Coating	$ Z _{f=0.006}$ ( $\Omega.cm^2$ )	Standard deviation ( $\Omega.cm^2$ )
DGEBA	$5.19 \times 10^{11}$	$4.97 \times 10^{11}$
DGEBA/7.5% lig.	$2.07 \times 10^{11}$	$6.24 \times 10^{10}$
DGEBA/15% lig.	$1.16 \times 10^{11}$	$5.65 \times 10^{10}$
DGEBA/30% lig.	$5.82 \times 10^9$	$1.71 \times 10^8$
CTE	$1.58 \times 10^9$	$2.08 \times 10^8$

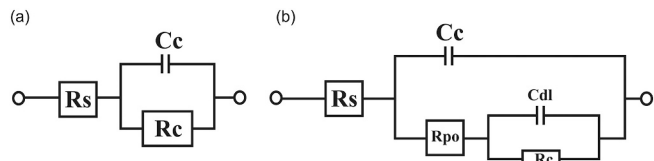


Fig. 9. (a) Randle model and (b) model for corroded metal substrate of EEC for carbon steel.

capacitance,  $R_{po}$  is the pore resistance and  $C_{dl}$  is the capacitance of the electrical double layer at the interface between the coating and the metal [4].

For the DGEBA, DGEBA/7.5% Lignin and DGEBA/15% Lignin coatings the Randle model (Fig. 9(a)) was used, this model indicates that the electrolyte was prevented from reaching the metallic surface by the barrier action of the coatings [36]. While for the DGEBA/30% Lignin and CTE coatings, the model indicated in Fig. 9(b) was used, indicating that the electrolyte has already reached the metallic surface through the pores of the coatings [36]. The average values of  $R_c$  calculated in relation to different immersion times are shown in Fig. 10.

The  $R_c$  values represented in Fig. 10 show that all coatings showed high values of resistance to polarization over the seven days of immersion in 3.5% NaCl solution. It is worth noting that the DGEBA, DGEBA/7.5% Lignin and DGEBA/15% Lignin coatings showed the best corrosion resistance performance, while the CTE coating had the worst performance, thus showing that the coatings with added lignin, except DGEBA/30% Lignin, which showed unsatisfactory results in relation to resin curing, can be used as a substitute for CTE coating.

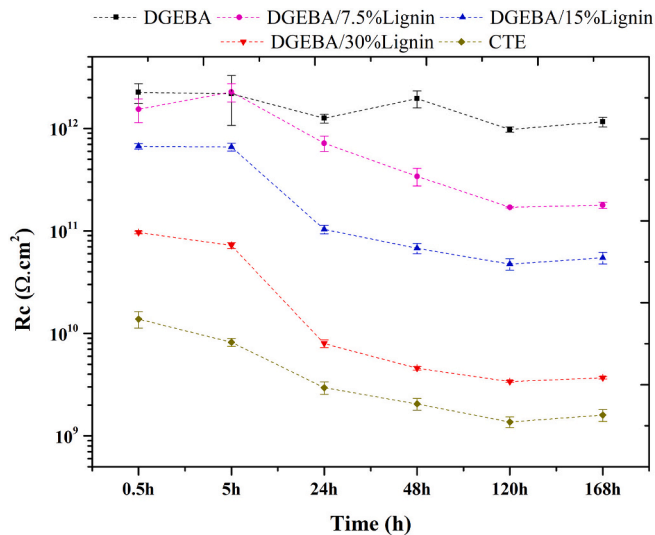


Fig. 10. Variation of  $R_c$  at low frequency (0.006 Hz) with time for the studied coatings.

### 3.7. Adhesion test

The results for the pull-off tensile strength (POTS) are shown in Fig. 11.

Considering the standard deviation of the POTS measurements, except for the CTE coating, all coatings showed similar values of tensile strength, indicating that the addition of lignin did not have negative effects in this aspect. The CTE coating showed the worst performance in this test, with an average tensile strength of 5.5 MPa, 33% lower than the second worst tensile strength value (DGEBA/30%Lignin coating). These results indicate that DGEBA and all DGEBA/Lignin epoxy coatings are able to withstand higher stress than the CTE coating without detaching from the metallic substrate.

Regarding the nature of the failure (Fig. 12), the adhesive failure was predominant at all the coatings, which occurs when there is a separation between two layers (A/B – coating/metallic substrate, B/Y – coating/adhesive glue, Y/Z - adhesive glue/dolly). A/B adhesive failure is undesirable, as it indicates that there was no good adhesion between the coating and the metallic substrate. However, regarding DGEBA/30%

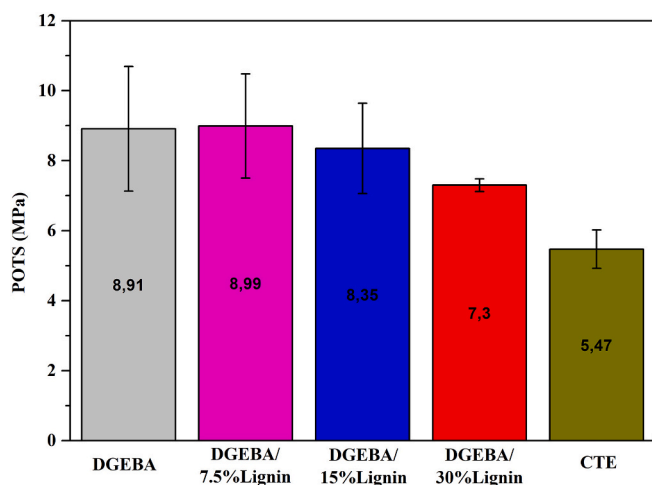


Fig. 11. Pull-off measures according to ASTM D 4541.

lignin coating, the coatings showed this type of failure with very similar values, indicating similarity between these coatings. It was also possible to observe that the type B cohesive failure remained practically the same in the coatings DGEBA, DGEBA/7.5% Lignin and DGEBA/15% Lignin and there was an increase of this type of failure in the DGEBA/30% Lignin coating. This type of failure is related to a good adhesion between coating and substrate, being the most common type for epoxy paint. Failures B/Y and Y/Z indicate that the tension applied during the test was not sufficient to promote the rupture between the coating and the metallic substrate, therefore, the metal remains protected by the coating in the areas related to these types of failures.

Therefore, it is possible to conclude that the DGEBA/Lignin coatings presented satisfactory performance relative to the tensile strength of the adhesion test, presenting values superior to the CTE coating and similar to the DGEBA coating. This result is very important as it indicates that DGEBA/Lignin coatings minimize the advance of corrosion under the film more efficiently than the CTE coating. Also indicating that lignin can be used as an additive in epoxy resins without compromising its adhesive properties.

#### 4. Conclusions

Epoxy resins with lignin addition were developed and, in comparison with epoxy resin without lignin addition and the CTE coating, it was concluded that:

- The addition of lignin in concentrations of 7.5 and 15% to the epoxy resin did not influence the curing process of the coatings and improved the thermal performance of the resin, since the glass transition temperature ( $T_g$ ) increased with the inclusion of lignin. The addition of 30% lignin resulted in the inefficiency of the resin curing process, negatively influencing the thermal results of this resin.
- The addition of acetylated lignin provided full UV absorption to the coatings, which can avoid photodegradation of these materials, making them more suitable to applications that require exposure to UV radiation.
- The results of EIS indicated that the addition of lignin to the epoxy resin, in the concentrations of 7.5 and 15%, did not significantly modify the value of the coatings impedance modulus, which are higher than the value of the CTE coating, ensuring the protection performance against corrosion of the metallic substrate.

These results indicate that DGEBA/7.5% AKL and DGEBA/15% AKL are potential substitutes to CTE coatings and promising materials to be used as organic coatings, since they presented excellent UV-blocker properties and protection against corrosion of carbon steel substrates. Further studies will be conducted in order to obtain more information about the behavior of these coatings when subjected to broader and long-term tests.

#### CRedit authorship contribution statement

- **Otilio B. F. Diógenes:** Writing – Original Draft/Investigation
- **Davi R. de Oliveira:** Writing – Original Draft/Investigation
- **Lucas R. R. da Silva:** Writing – Original Draft/Investigation
- **Ítalo Gomes Pereira:** Investigation
- **Selma Elaine Mazzetto:** Funding Acquisition/Project Administration
- **Walney S. Araujo:** Funding Acquisition/Writing – Review & Editing/Supervision/Conceptualization

	DGEBA	DGEBA/ 7.5%Lignin	DGEBA/ 15%Lignin	DGEBA/ 30%Lignin	CTE
DOLLY					
STEEL					
FAILURE	A/B - 36% B - 9% B/Y - 55%	A/B - 40% B - 9% B/Y - 51%	A/B - 40% B - 11% Y/Z - 49%	B - 40% B/Y - 60%	A/B - 34% B - 47% Y/Z - 19%

Fig. 12. Type of Failure after Pull-off test.



- **Diego Lomonaco:** Funding Acquisition/Writing – Review & Editing/Supervision/Conceptualization

### Declaration of competing interest

The authors declare that they have no known competing financial interests or personal relationships that could have appeared to influence the work reported in this paper.

### Acknowledgments

The authors acknowledge Brazilian agencies Conselho Nacional de Desenvolvimento Científico e Tecnológico (CNPq) (407291/2018-0), Coordenação de Aperfeiçoamento de Pessoal de Nível Superior (CAPES) (Finance Code 001) and Fundação Cearense de Apoio ao Desenvolvimento Científico e Tecnológico (Funcap) for the financial support.

### Data availability

The raw/processed data required to reproduce these findings cannot be shared at this time as the data also forms part of an ongoing study.

### References

- Y. Wu, J. Yu, W. Zhao, C. Wang, B. Wu, G. Lu, Investigating the anti-corrosion behaviors of the waterborne epoxy composite coatings with barrier and inhibition roles on mild steel, *Prog. Org. Coat.* 133 (Aug. 2019) 8–18.
- L.K. Aggarwal, P.C. Thapliyal, S.R. Karade, Anticorrosive properties of the epoxy-cardanol resin based paints, *Prog. Org. Coat.* 59 (1) (2007) 76–80.
- Z. Feng, et al., Salt crystallization-assisted degradation of epoxy resin surface in simulated marine environments, *Prog. Org. Coat.* 149 (September) (2020), 105932.
- S.D. Jagtap, S.P. Tambe, R.N. Choudhari, B.P. Mallik, Mechanical and anticorrosive properties of non toxic coal-tar epoxy alternative coating, *Prog. Org. Coat.* 77 (2) (2014) 395–402.
- A. Ramaswami, R.G. Luthy, Mass transfer and bioavailability of PAH compounds in coal tar NAPL-slurry systems. 1. Model development, *Environ. Sci. Technol.* 31 (8) (1997) 2260–2267.
- A.C.L. Chiovatto, et al., Effects of substances released from a coal tar-based coating used to protect harbor structures on oysters, *Mar. Pollut. Bull.* 166 (May 2021), 112221.
- W. Thielemans, E. Can, S.S. Morye, R.P. Wool, Novel applications of lignin in composite materials, *J. Appl. Polym. Sci.* 83 (2) (Jan. 2002) 323–331.
- D.S. Bajwa, G. Pourhashem, A.H. Ullah, S.G. Bajwa, A concise review of current lignin production, applications, products and their environment impact, *Ind. Crop. Prod.* 139 (February) (2019), 111526.
- R. Yan, et al., Improved performance of dual-cured organosolv lignin-based epoxy acrylate coatings, *Compos. Commun.* 10 (Dec. 2018) 52–56.
- M.H. Hussin, A.A. Rahim, M.N. Mohamad Ibrahim, N. Brosse, Improved corrosion inhibition of mild steel by chemically modified lignin polymers from *Elaeis guineensis* agricultural waste, *Mater. Chem. Phys.* 163 (2015) 201–212.
- S.J. Marciano, F. Avelino, L.R.R. da Silva, S.E. Mazzetto, D. Lomonaco, Microwave-assisted phosphorylation of organosolv lignin: new bio-additives for improvement of epoxy resins performance, *Biomass Convers. Biorefinery* (Oct. 2020), <https://doi.org/10.1007/s13399-020-01048-7>.
- F. Avelino, D.R. de Oliveira, S.E. Mazzetto, D. Lomonaco, Poly(methyl methacrylate) films reinforced with coconut shell lignin fractions to enhance their UV-blocking, antioxidant and thermo-mechanical properties, *Int. J. Biol. Macromol.* 125 (2019) 171–180.
- O. Gordobil, R. Herrera, M. Yahyaoui, S. Ilk, M. Kaya, J. Labidi, Potential use of kraft and organosolv lignins as a natural additive for healthcare products, *RSC Adv.* 8 (43) (2018) 24525–24533.
- W. Yang, et al., Role of lignin nanoparticles in UV resistance, thermal and mechanical performance of PMMA nanocomposites prepared by a combined free-radical graft polymerization/masterbatch procedure, *Compos. A Appl. Sci. Manuf.* 107 (2018) 61–69.
- S. Nikafshar, O. Zabihi, M. Ahmadi, A. Mirmohseni, M. Taseidifar, M. Naebe, The effects of UV light on the chemical and mechanical properties of a transparent epoxy-diamine system in the presence of an organic UV absorber, *Materials (Basel)*. 10 (2) (2017) 1–18.
- D.R. de Oliveira, F. Avelino, S.E. Mazzetto, D. Lomonaco, Microwave-assisted selective acetylation of Kraft lignin: acetic acid as a sustainable reactant for lignin valorization, *Int. J. Biol. Macromol.* 164 (2020) 1536–1544.
- F. Monteil-Rivera, L. Paquet, Solvent-free catalyst-free microwave-assisted acylation of lignin, *Ind. Crop. Prod.* 65 (2015) 446–453.
- D.R. De Oliveira, et al., Ecofriendly modification of acetosolv lignin from oil palm biomass for improvement of PMMA thermo-oxidative properties 45498 (2017) 1–8.
- W. Thielemans, R.P. Wool, Lignin esters for use in unsaturated thermosets: lignin modification and solubility modeling, *Biomacromolecules* 6 (4) (Jul. 2005) 1895–1905.
- O. Faix, Classification of lignins from different botanical origins by FT-IR spectroscopy, *Holzforchung* 45 (s1) (Jan. 1991) 21–28.
- D. Ye, et al., Selective aminolysis of acetylated lignin: toward simultaneously improving thermal-oxidative stability and maintaining mechanical properties of polypropylene, *Int. J. Biol. Macromol.* 108 (Mar. 2018) 775–781.
- D.W. van Krevelen, Some basic aspects of flame resistance of polymeric materials, *Polymer (Guildf)*. 16 (8) (1975) 615–620.
- L.R.V. Kotzebue, J.R. De Oliveira, J.B. Da Silva, S.E. Mazzetto, H. Ishida, D. Lomonaco, Development of fully biobased high-performance bis-benzoxazine under environmentally friendly conditions, *ACS Sustain. Chem. Eng.* 6 (4) (2018) 5485–5494.
- H. Abdollahi, A. Salimi, M. Barikani, A. Samadi, S. Hosseini Rad, A.R. Zanjani, Systematic investigation of mechanical properties and fracture toughness of epoxy networks: role of the polyetheramine structural parameters, *J. Appl. Polym. Sci.* 136 (9) (2019) 1–11.
- L.C. Over, E. Grau, S. Grelier, M.A.R. Meier, H. Cramail, Synthesis and characterization of epoxy thermosetting polymers from glycidylated organosolv lignin and bisphenol A, *Macromol. Chem. Phys.* 218 (4) (2017) 1–11.
- F. Avelino, K.T. Silva, S.E. Mazzetto, D. Lomonaco, Tailor-made organosolv lignins from coconut wastes: effects of green solvents in microwave-assisted processes upon their structure and antioxidant activities, *Bioresour. Technol. Reports* 7 (Sep. 2019), 100219.
- R. Yan, et al., Performance of UV curable lignin based epoxy acrylate coatings, *Prog. Org. Coat.* 116 (November 2017) (2018) 83–89.
- F. Ferdosian, Z. Yuan, M. Anderson, C. Charles, Journal of analytical and applied pyrolysis thermal performance and thermal decomposition kinetics of lignin-based epoxy resins, *J. Anal. Appl. Pyrolysis* 119 (2016) 124–132.
- S. Ma, et al., Synthesis and properties of a bio-based epoxy resin with high epoxy value and low viscosity, *ChemSusChem* 7 (2) (Feb. 2014) 555–562.
- L.R.R. da Silva, et al., Development of BPA-free anticorrosive epoxy coatings from agroindustrial waste, *Prog. Org. Coat.* 139 (July) (2020), 105449.
- Y. Qian, X. Qiu, S. Zhu, Lignin: a nature-inspired sun blocker for broadspectrum sunscreens, *Green Chem.* 17 (1) (2015) 320–324.
- Y. Qian, X. Qiu, S. Zhu, Sunscreen performance of lignin from different technical resources and their general synergistic effect with synthetic sunscreens, *ACS Sustain. Chem. Eng.* 4 (7) (2016) 4029–4035.
- S. Wang, et al., Green synthesis of graphene with the assistance of modified lignin and its application in anticorrosive waterborne epoxy coatings, *Appl. Surf. Sci.* 484 (September 2018) (2019) 759–770.
- I.C.P. Margarit-Mattos, F.A.R. Agura, C.G. Silva, W.A. Souza, J.P. Quintela, V. Solymosy, Electrochemical impedance aiding the selection of organic coatings for very aggressive conditions, *Prog. Org. Coat.* 77 (12) (2014) 2012–2023.
- M. Mahdavian, M.M. Attar, Another approach in analysis of paint coatings with EIS measurement: phase angle at high frequencies 48 (2006) 4152–4157.
- E. Akbarinezhad, M. Bahremandi, H.R. Faridi, F. Rezaei, Another approach for ranking and evaluating organic paint coatings via electrochemical impedance spectroscopy, *Corros. Sci.* 51 (2) (2009) 356–363.